RSC Advances

PAPER



Cite this: *RSC Adv.*, 2024, **14**, 3841

# Fluorescence photobleaching and recovery of fluorescein sodium in carbomer film

Yung-Sheng Lin, [a] Hao-Yan Chen[a] and Yih-Pey Yang *[b]

Received 21st December 2023
Accepted 20th January 2024

DOI: 10.1039/d3ra08718b

rsc.li/rsc-advances

This study investigated fluorescence photobleaching and the recovery of fluorescein sodium (FS)-loaded carbomer films. To mitigate errors caused by the self-quenching effect, the experiments were conducted at FS concentrations of 0.1, 0.5, and 1 wt%. The results revealed a nonlinear relationship between fluorescence intensity and FS concentration (0.1–1 wt%). Moreover, the degree and rate of photobleaching increased with FS concentration. The recovery level and recovery rate exhibited contrasting relationships with FS concentration. Higher FS concentrations were associated with a longer recovery time, which can be attributed to the prolonged irradiation, resulting in a bleached region that was larger than the initially irradiated area.

## Introduction

Fluorescence technology plays a pivotal role in the field of biomedical research.[1,2] A common challenge in using this technology is photobleaching, which affects the effectiveness of fluorescence imaging in clinical medicine. Understanding photobleaching kinetics is essential for effectively addressing its occurrence. Furthermore, the study of photobleaching can shed light on molecular mobility and diffusion phenomena. This knowledge is crucial for overcoming the aforementioned challenges and enhancing the utility of fluorescence imaging techniques in clinical applications.

Fluorescence recovery after photobleaching (FRAP) is an essential technique for studying molecular mobility and diffusion phenomena across various scientific domains. FRAP is widely used to measure slow diffusion[3,4] in various contexts, including high-viscosity solutions,[5–7] colloidal systems,[8,9] thin films,[10–13] live cells,[14–17] and others.[18,19] The effectiveness of FRAP in measuring molecular diffusion is influenced not only by the molecules themselves but also by their environmental medium. FRAP can also be used to explore the microstructural characteristics underlying the resolution of fluorescence microscopy.

Notably, the motion of fluorescent molecules in aqueous solutions differs considerably from their motion in biological cell tissues. In cell tissues, in addition to Brownian motion, fluorescent molecules interact with the cellular environment, which influences their diffusion behavior.[20–25] Relevant studies have attempted to extract information about the microstructural properties of the cellular environment or factors such as binding[14,21–24] from anomalous diffusion.

In scenarios where excessive interference hinders the application of appropriate diffusion theory models to measure the motion of molecules, some researchers have applied the half-time for recovery as a substitute for diffusion coefficients to quantify molecular motion.[20–22] Studies applying FRAP have typically employed short photobleaching times and small photobleached volumes to minimize experimental interference, enabling the application of mathematical models of diffusion coefficients.[26,27] However, in clinical applications and biomedical research, photobleaching engendered by prolonged fluorescence excitation is a more prevalent problem.[28,29]

The application of fluorescence imaging in clinical medicine introduces challenges related to prolonged fluorescence excitation; this is because both photobleaching and recovery phenomena can influence the interpretation of fluorescence signals, which may lead to misdiagnoses or inaccuracies in surgical procedures. However, the use of FRAP for conducting long-term photobleaching experiments to investigate molecular dynamics is relatively uncommon. Our previous study involved conducting extended photobleaching experiments using a self-constructed laser-induced fluorescence system,[2] but we did not explore the subsequent recovery kinetics.

To clearly understand photobleaching and FRAP in clinical medicine, the present study employed carbomer films as biomimetic substrates and explored the photobleaching and recovery kinetics of fluorescein sodium (FS) that was loaded within these carbomer films.

## Experimental section

### Preparation of FS-loaded carbomer films

We mixed 2 g of 1 wt% carbomer with 2 g of 0.001, 0.005, 0.01, 0.02, and 0.03 wt% FS solutions separately in a 5 cm-diameter plastic Petri dish. These five homogeneously mixed FS–

[a]Department of Chemical Engineering, National United University, Taiwan
[b]Department of Biomechatronic Engineering, National Ilan University, Taiwan

carbomer solutions were then dried in an oven at 50 °C for 12 h, resulting in the formation of 0.1, 0.5, 1, 2, and 3 wt% FS-loaded carbomer films. These steps were all conducted in a light-shielded environment. A compact fluorescence detection system comprising a fiber-coupled light-emitting diode and photodiode sensor[2] was used to measure the photobleaching and recovery dynamics of these samples at a constant temperature (25 °C). The 10 minutes irradiation of 470 nm LED was applied for photobleaching and then recovery observation was followed at predetermined time points until reaching plateau of fluorescence intensity.

### Photobleaching and recovery model

We used a photobleaching model based on the exponential decay framework outlined in a previous study.[2] Fig. 1 illustrates the framework; in this framework, the exponential decay of fluorescence intensity starts at the initial intensity $I_{original}$ and progresses to the fluorescence intensity $I_0$ at the conclusion of the bleaching process ($t_0$). Subsequently, the fluorescence recovery process initiates at $t_0$. However, the fluorescence intensity does not achieve complete recovery, ultimately converging toward $I_{plateau}$. All fluorescence intensity values are normalized with respect to $I_{original}$ to obtain the normalized intensity for further analysis.

## Results and discussion

Fig. 2 illustrates the fluorescence intensity of the carbomer films loaded with FS at varying concentrations. The results indicate that the fluorescence intensity initially increases with the FS concentration, yet undergoes a subsequent inversion and declines beyond a concentration threshold of 1 wt%. This can be attributed to the phenomenon of self-quenching, which resulted in a decrease in fluorescence intensity at FS concentrations of 2 and 3 wt%. This observation is consistent with the findings of previous research, which attributed self-quenching to collisions between excited fluorophores, the formation of nonfluorescent dimers, and energy transfer to the nonfluorescent dimers.[30] Additionally, a nonlinear correlation was observed between fluorescence intensity and FS concentrations ranging from 0.1 to 1 wt%; this demonstrates that the number of fluorescent molecules exerted a multiplicative effect on fluorescence intensity. To mitigate potential errors in our subsequent recovery experiments due to the self-quenching effect, we conducted our experiments by using FS concentrations that were below the critical concentration; specifically, we used the FS concentrations of 0.1, 0.5, and 1 wt%.

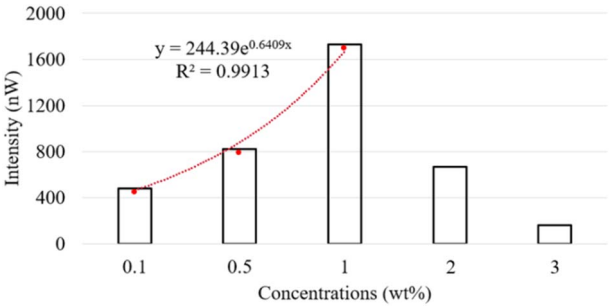


Fig. 2 Effects of FS concentration on fluorescence intensity of FS-loaded carbomer films.

We conducted a 10 min photobleaching experiment on the FS-loaded carbomer films, and the resulting dynamic normalized fluorescence intensity values are illustrated in Fig. 3. As demonstrated in this figure, a higher FS concentration was associated with a greater degree of photobleaching. This finding is attributable to the reversal of the multiplicative effect of fluorescent molecule concentration on fluorescence intensity (Fig. 2). Another possible explanation for this finding is that the increased FS concentration resulted in a higher encounter probability for the self-quenching process.[31] Consequently, when subjected to identical irradiation intensity levels and durations, the highly concentrated fluorescent molecules experienced a more pronounced bleaching effect than did the molecules with lower concentrations.

In our previous study,[2] we used a double-exponential decay model for an optimal numerical analysis of the photobleaching process. Although the double-exponential decay model provided excellent optimization fits, we noted a substantial difference (up to a factor of 20) in the two kinetic constants within the double-exponential component. This discrepancy

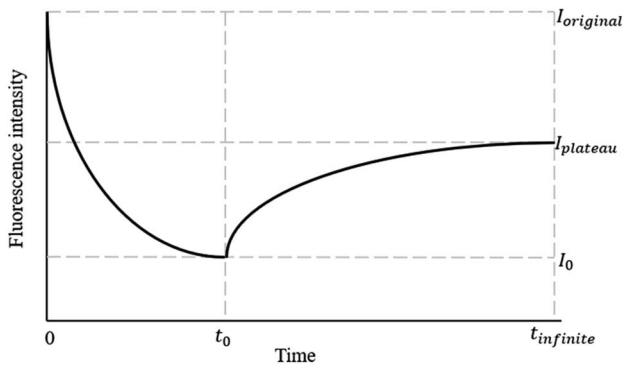


Fig. 1 Dynamic fluorescence intensity in photobleaching and recovery processes.

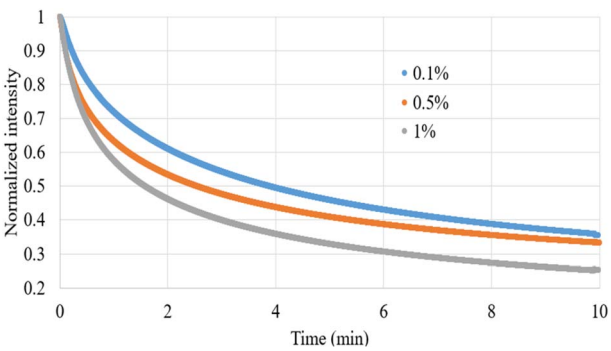


Fig. 3 Dynamic normalized intensity of FS-loaded carbomer films during a 10 min photobleaching process.

Table 1 Results of optimal analysis of photobleaching, as derived using $I(t) = A + Be^{-kt}$

| Con. (wt%) | $A$ | $B$ | $k$ (min$^{-1}$) | $R^2$ |
|---|---|---|---|---|
| 0.1 | 0.3650 | 0.5552 | 0.3849 | 0.9898 |
| 0.5 | 0.3507 | 0.5104 | 0.4919 | 0.9795 |
| 1 | 0.2745 | 0.5863 | 0.5542 | 0.9779 |

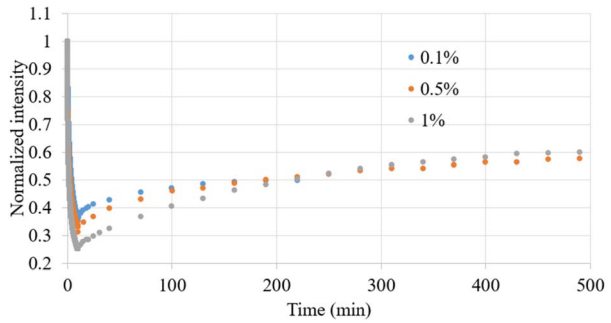


Fig. 4 Dynamic normalized intensity observed after photobleaching and recovery of carbomer films containing various FS concentrations by 10 min irradiation.

Table 2 Results of best fit in $I(t) = I_0 + (I_{plateau} - I_0)(1 - e^{-kt})$

| Wt (%) | $I_0$ (%) | $I_{plateau}$ (%) | $r$ (%) | $k$ (min$^{-1}$) | $t_{1/2}$ (min) | $R^2$ |
|---|---|---|---|---|---|---|
| 0.1 | 35.46 | 49.95 | 22.45 | 0.0211 | 32.92 | 0.98 |
| 0.5 | 31.19 | 57.01 | 38.40 | 0.0070 | 99.02 | 0.98 |
| 1 | 25.20 | 60.00 | 46.52 | 0.0053 | 131.28 | 0.99 |

suggested that the influence of one of the exponential terms was negligible. Consequently, the present study used a single-exponential decay model for an optimal analysis of photobleaching kinetics. The analysis results are presented in Table 1, indicating that the derived correlation coefficients consistently exceeded 0.97. In this table, the constant $A$ represents the fluorescence intensity after photobleaching, with a lower value indicating a higher degree of photobleaching, and $k$ represents the photobleaching rate constant. The optimized numerical values demonstrate that in addition to irradiation intensity and time, the concentration of fluorescent molecules substantially affects the degree of photobleaching. Moreover, the $k$ values revealed that during the photobleaching process, higher FS concentrations were associated with a greater degree of photobleaching compared with lower FS concentrations. In summary, both the degree and rate of photobleaching increased with the FS concentrations.

After the bleaching process, we conducted fluorescence recovery measurements. Fig. 4 presents the dynamic normalized intensity in a recovered carbomer film containing various concentrations of FS after a 10 min irradiation process. The fluorescence recovery processes displayed similar patterns after similar irradiation durations. To quantify the fluorescence recovery processes, a recovery curve was plotted according to a previously reported model,[16] as shown in Table 2. The calculated $I_0$ obtained from the recovery process, representing the fluorescence intensity after photobleaching, exhibited a slight discrepancy when compared with the theoretical value of $A$ for the bleaching endpoint in Table 1, which was derived in the calculation of the effects of the bleaching process. However, according to both Tables 1 and 2, the degree of bleaching increased with the FS concentrations. The final normalized fluorescence intensity $I_{plateau}$ obtained from the analysis of the recovery processes confirmed that complete recovery was not achievable. The assumption underlying the recovery processes was that different FS concentrations would ultimately return to the same proportion of their original concentration. Due to the nonlinear relationship between fluorescence intensity and FS concentration, the final normalized fluorescence intensity $I_{plateau}$ increased with the FS concentrations. The recovery level $r$ (%) was derived using the following equation: $(I_{plateau} - I_0)/(1 - I_0) \times 100\%$. We observed that higher FS concentrations were associated with more pronounced recovery levels. This indicates that the nonlinear increase in fluorescence intensity with FS concentration overshadows the bleaching effect associated with the increase in FS concentration.

We also calculated the kinetic constant $k$, which represents the recovery rate, in our simulation of the recovery process, and the results revealed distinct results from those observed for the recovery level $r$. Specifically, as indicated in Table 2, the recovery rate decreased as the FS concentration increased. This relationship can be expressed as follows: $t_{1/2} = (\ln 2)/k$, where $t_{1/2}$ represents the half-time of recovery. This expression indicates that higher FS concentrations correspond to longer recovery times. Accordingly, $r$ and $k$ exhibited contrasting relationships with FS concentration. According to the literature,[26] the recovery rate is inversely related to the size of the bleached region. We hypothesized that during photobleaching, unbleached FS molecules near the irradiated area migrate into the irradiated region, while the bleached molecules within the region simultaneously disperse outward. This dynamic creates a phenomenon where the region outside the irradiated area seems to experience similar bleaching, giving the appearance of an expansion of the original irradiated zone. An increase in FS concentration can result in a more pronounced concentration disparity between the interior and exterior of the irradiated region during bleaching. This disparity can accelerate the relative movement of molecules inside and outside the irradiated area, consequently amplifying the affected region beyond the originally bleached area.

## Conclusions

In clinical medicine, fluorescence imaging techniques require prolonged exposure to accurately monitor fluorescence signals. This study used carbomer films as biomimetic substrates to investigate the photobleaching and recovery kinetics of FS molecules. The results demonstrate a nonlinear relationship between fluorescence intensity and FS concentration. Moreover, the results reveal that under extended exposure durations, the concentration of fluorescent molecules significantly influenced

the photobleaching rate, photobleaching degree, recovery level, and recovery rate. Notably, the recovery rate decreased as the FS concentration increased, marking a deviation from the conventional pure diffusion phenomenon.

## Author contributions

Conceptualization: Yung-Sheng Lin and Yih-Pey Yang; investigation: Yung-Sheng Lin and Yih-Pey Yang; data curation: Hao-Yan Chen; funding acquisition and supervision: Yung-Sheng Lin and Yih-Pey Yang; writing – original draft: Yung-Sheng Lin and Yih-Pey Yang; writing – review and editing: Yung-Sheng Lin and Yih-Pey Yang. All authors have read and agreed to the published version of the manuscript.

## Conflicts of interest

There are no conflicts to declare.

## Acknowledgements

This study received funding from the National Science and Technology Council, Taiwan (112-2622-E-239-004).

## Notes and references

1 J. W. Lichtman and J. A. Conchello, *Nat. Methods*, 2005, **2**, 910–919.
2 C.-J. Weng, C.-H. Lien, C.-Y. Chen, C.-H. Yuh, C.-J. Chen and Y.-S. Lin, *Measurement*, 2018, **128**, 84–88.
3 E. Van Keuren and W. Schrof, *Macromolecules*, 2003, **36**, 5002–5007.
4 K. Majerczak, Z. Shi, Z. Zhang and Z. J. Zhang, *Prog. Org. Coat.*, 2023, **185**, 107833.
5 A. C. Geiger, C. J. Smith, N. Takanti, D. M. Harmon, M. S. Carlsen and G. J. Simpson, *Biophys. J.*, 2020, **119**, 737–748.
6 S. Khandai and S. S. Jena, *J. Colloid Interface Sci.*, 2017, **505**, 196–205.
7 S. Seiffert and W. Oppermann, *J. Microsc.*, 2005, **220**, 20–30.
8 S. Khandai, R. A. Siegel and S. S. Jena, *Colloids Surf., A*, 2020, **593**, 124618.
9 A. A. Moud, *ACS Biomater. Sci. Eng.*, 2022, **8**, 1028–1048.
10 J. Hauth, J. Chodorski, A. Wirsen and R. Ulber, *Biophys. J.*, 2020, **118**, 2354–2365.
11 J. D. Bryers and F. Drummond, *Biotechnol. Bioeng.*, 1998, **40**, 462–473.
12 D. Sustr, C. Duschl and D. Volodkin, *Eur. Polym. J.*, 2015, **68**, 665–670.
13 P. Jonsson, M. P. Jonsson, J. O. Tegenfeldt and F. Hook, *Biophys. J.*, 2008, **95**, 5334–5348.
14 C. A. Day and M. Kang, *Membranes*, 2023, **13**, 492.
15 M. Shetty, D. E. Bolland, J. Morrell, B. D. Grove, J. D. Foster and R. A. Vaughan, *Curr. Res. Physiol.*, 2023, **6**, 100106.
16 S. Takeshi, C. G. Pack and R. D. Goldman, *Methods Mol. Biol.*, 2016, **1411**, 99–111.
17 C. A. Day, L. J. Kraft, M. Kang and A. K. Kenworthy, *Curr. Protoc. Cytom.*, 2012, **62**(1), 19.
18 C. Chen, D. Li, J. Li, X. Chen, W. Wei and X. Wang, *Food Struct.*, 2022, **31**, 100251.
19 J. Floury, M. N. Madec, F. Waharte, S. Jeanson and S. Lortal, *Food Chem.*, 2012, **133**, 551–556.
20 D. Dey, A. Nunes-Alves, R. C. Wade and G. Schreiber, *iScience*, 2022, **25**, 105088.
21 D. T. Brown, T. Izard and T. Misteli, *Nat. Struct. Mol. Biol.*, 2006, **13**, 250–255.
22 M. A. Ozturk and R. C. Wade, *Biochim. Biophys. Acta, Gen. Subj.*, 2020, **1864**, 129653.
23 B. L. Sprague, R. L. Pego, D. A. Stavreva and J. G. McNally, *Biophys. J.*, 2004, **86**, 3473–3495.
24 A. M. Alexander and S. D. Lawley, *Biophys. J.*, 2022, **121**, 3795–3810.
25 D. Dey, S. Marciano, A. Nunes-Alves, V. Kiss, R. C. Wade and G. Schreiber, *J. Mol. Biol.*, 2021, **433**, 166898.
26 N. Loren, J. Hagman, J. K. Jonasson, H. Deschout, D. Bernin, F. Cella-Zanacchi, A. Diaspro, J. G. McNally, M. Ameloot, N. Smisdom, M. Nyden, A. M. Hermansson, M. Rudemo and K. Braeckmans, *Q. Rev. Biophys.*, 2015, **48**, 323–387.
27 T. K. L. Meyvis, S. C. De Smedt, P. Van Oostveldt and J. Demeester, *Pharm. Res.*, 1999, **16**, 1153–1162.
28 T. S. Mang, T. J. Dougherty, W. R. Potter, D. G. Boyle, S. Somer and J. Moan, *Photochem. Photobiol.*, 1987, **45**, 501–506.
29 K. L. Lou, P. Y. Wang, R. Q. Yang, Y. Y. Gao, H. N. Tian, Y. Y. Dang, Y. Li, W. H. Huang, M. Chen, X. L. Liu and G. J. Zhang, *Nanomedicine*, 2022, **43**, 102555.
30 W. Bae, T.-Y. Yoon and C. Jeong, *PLoS One*, 2021, **16**, e0247326.
31 L. Song, R. P. M. van Gijlswijk, I. T. Young and H. J. Tanke, *Cytometry*, 1997, **27**, 213–223.